# ANALYTIC METHODS FOR CODE COMPARISON EVALUATION AND TARGET TEMPERATURE PREDICTION

William L. Foley and Vincent J. Velten
Target Recognition Technology Branch
Avionics Directorate, Wright Laboratory
Wright Patterson Air Force Base
Dayton Ohio

## ABSTRACT

The variety of codes used for prediction of target temperatures suggests that a standard be devised which might be useful for comparing the prediction accuracy of various codes. A method is proposed based upon an analytic solution of the heat transfer equation. Such an approach appears to offer a high accuracy solution from which the temperature prediction can be obtained directly for any location on the target at any point during the thermal history. Numerical methods require solutions based upon thermal history over the volumetric extent of the target. These factors are inherent in the analytic solution so that predictions can be made directly at any given time and location on the target. Furthermore, an analytic solution could be particularly useful for temperature prediction against targets with thin, highly conductive surfaces. It is here that numerical methods can break down or are forced into approximations which compromise resultant accuracy.

An analytic formulation is described in this paper which is based upon a 1D heat transfer model that can be employed against a simple target configuration. The boundary conditions for driving the model include typical solar loading, convective, and radiative heat exchange factors as derived from algorithms found in currently available prediction codes. Usefulness of the model for temperature prediction against a target with thin, highly conductive surfaces is demonstrated as well as the utility of the model for code comparison. Results illustrate the differences in temperature prediction as a function of assumed boundary conditions and also with numerical prediction based upon isothermal facet conditions.

## 1.0 Introduction and background

The increased use of thermal sensors for target acquisition, recognition, and identification has necessitated that effective means be employed to predict operational performance. Simulation is a key means of making such assessments and must be capable of use in both system design and mission deployment. An end to end simulation includes a representation of sensor performance characteristics, atmospheric influence, and temperature profile predictions for both target and background.

The prediction of signature profiles from the target is based upon a combination of geometric modeling, algorithms to represent environmental influences, and solving the heat transfer equations to determine target surface temperatures and radiances. The target representation is typically in the form of a facetized characterization of the surface geometry. Individual facets are considered isothermal and a heat balance equation is solved for each facet in the form of radiative, solar, and convective exchanges which form the boundary conditions for each facet. Solar loading involves direct solar radiation, sky radiation and ground reflective radiation. Radiation exchange includes the contribution of both long wavelength sky and Earth background for each facet. Convective exchange is typically a simplified empirical formulation considered most practical for the given target geometry. Radiative and conductive exchanges within the target are also part of the heat exchange process but certain of these may be ignored under most conditions.

Numerical methods are employed to solve the heat transfer equation as there are no practical alternatives for complex boundary conditions. Both explicit and implicit methods can be employed with the implicit method preferred since it is unconditionally stable over all thermal inertia conditions.

In conjunction with new model formulation, or in the evaluation of existing modeling approaches, issues of target modeling fidelity, algorithms employed for temperature prediction, and numerical solution methods must be addressed. Simplified target modeling, together with an analytic method for temperature prediction, appears to offer a highly accurate and stable method for evaluating and comparing algorithms or accuracy of numerical methods. Tractability of analysis is also facilitated with simplified geometric representations. The analytic approach offered herein can be used in conjunction with signature prediction for highly complex targets and is potentially more accurate where target features are composed of thin, low inertia materials. An approach is presented in this paper which is believed to be consistent with these observations.

## 2. **Modeling approach**

To illustrate our approach the problem of temperature prediction of a thin slab whose transverse dimensions are large relative to the thickness is considered. We assume that the dominant mode of heat exchange is normal to the material surface so that only 1D heat flow need be considered. Thin slabs may be connected to represent target features which in a simple form would consist of a box (or more precisely, a cube). If box dimensions are sufficiently large then facet to facet conduction can be safely ignored along with radiation exchange between facets in the box interior. However both long and short wavelength radiation exchanges with the environment external to the box are certainly significant and must be considered in the heat balance equation.

Although a box is a simple feature, the surface geometry contains significant discontinuities to challenge a prediction model. Each surface can be exposed to a significantly different external environment which must in turn be considered in the model formulation. For the purpose of this paper it will be assumed that sky and ground each are of uniform temperature. The vertical facets then exchange radiation with both the sky and ground whereas the top surface views only the sky. The scenario is then as shown in Figure 1.

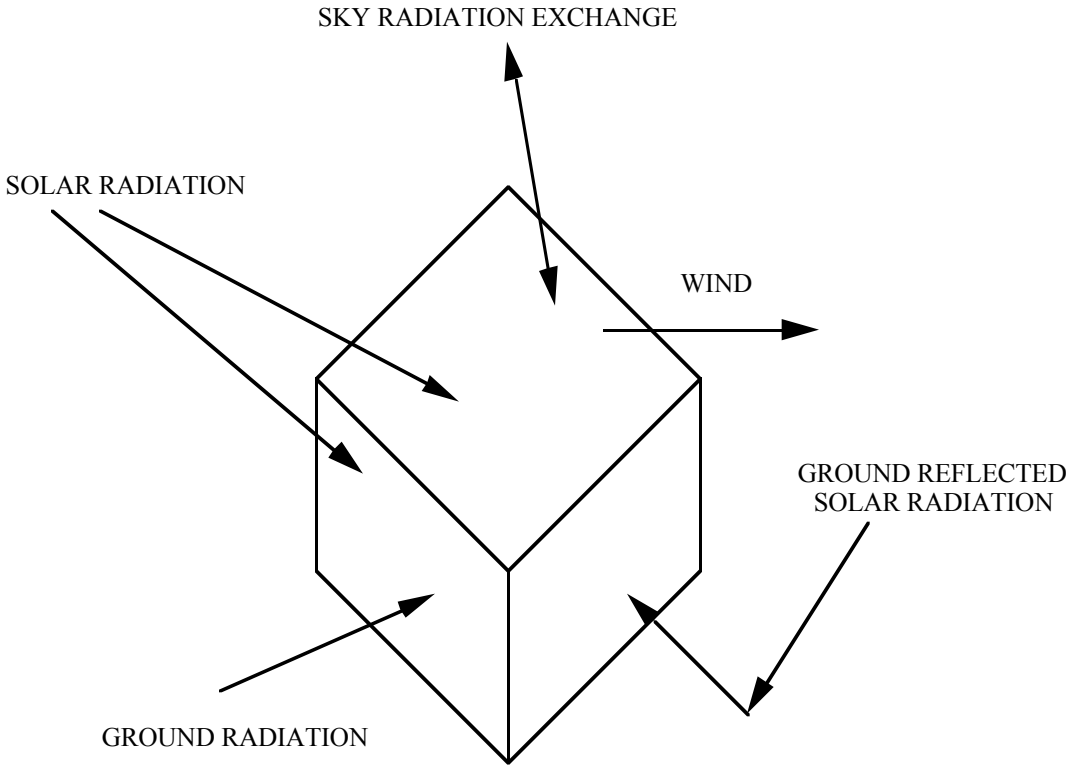


Figure 1. Modeling Scenario. Each face of the cube is 3 $m^2$ in area and 1 cm thick.

The analytic formulation is developed through the solution of the classical 1D heat conductive equation subject to radiative solar and convective loading conditions on the external and internal boundaries of each facet. For the general form of the solution proposed here, it will be assumed that the internal boundary can interact with internal environment through radiative and free convective exchange. The internal environment can be controlled or floating with respect to changes in external conditions. The heat exchange mechanisms must then be quantified which for the purposes herein is done using algorithms from existing thermal prediction codes. The generic form of these algorithms for the solar, radiative and convective loading are as given in Equations (1), (2), and (3) respectively.

$$Q_S = S_D \cos(\phi) + S_\infty V_\infty + S_G V_G \quad [\mathrm{W} / \mathrm{m}^2] \tag{1}$$

$S_D$ = direct solar flux [W / $m^2$]
$S_\infty$ = sky diffuse radiation flux [W / $m^2$]
$S_G$ = ground diffuse radiation flux [W / $m^2$]

$V_\infty$ = view factor surface-to-sky
$V_G$ = view factor surface-to-ground
$\phi$ = interior angle between surface normal and solar direction

$$Q_R = \sigma\left(\left(\varepsilon_\infty T_\infty^4 - \varepsilon_S T_S^4\right)V_\infty + \left(\varepsilon_G T_G^4 - \varepsilon_S T_S^4\right)V_G\right) \quad [\mathrm{W/m^2}] \tag{2}$$

$\sigma$ = Stephan-Boltzman constant
$T_\infty$ = sky temperature [K]
$T_G$ = ground temperature [K]
$T_S$ = facet surface temperature [K]
$\varepsilon_\infty$ = sky emmissivity
$\varepsilon_G$ = ground emmissivity
$\varepsilon_S$ = facet emmissivity

$$Q_C = h\left(T_S - T_A\right) \quad [\mathrm{W/m^2}] \tag{3}$$

$$h = c_1 + c_2 v_w \quad [\mathrm{W/m^2 \cdot K}] \tag{3a}$$

$T_A$ = air temperature [K]
$v_w$ = wind velocity [m / s]
$h$ = convective heat transfer coefficient
$c_1, c_2$ = constants of fit

Determining the surface temperature of facets through analytic means is seriously impeded with the presence of higher order coupling terms as is evident from Equation (2). However it can be shown that if the difference between surface temperatures and air temperature is reasonably bounded, radiation exchange can be linearized. This is illustrated in Figure 2.

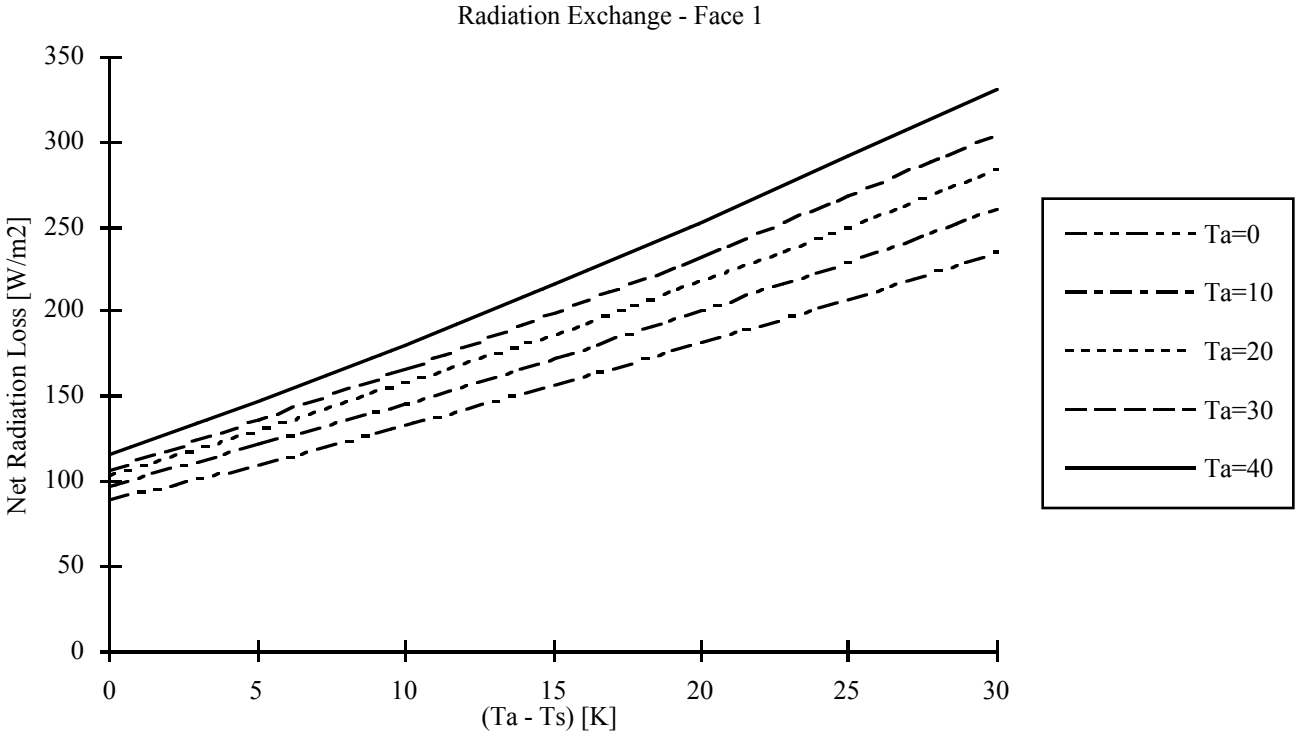


Figure 2: The approximately linear relationship between net radiation exchange and surface to environment $\Delta T$ for small values of $\Delta T$.

The above curves are based upon an assumed relative humidity of 50 percent. The total radiation can then be expressed in terms of a slope and intercept whose values depend upon air temperature, relative humidity, and sky and ground view factors. The sky temperature term in Equation (2) is expressed in terms of ambient air temperature and the result is incorporated into the radiation curves above. It is this effect that causes the non-zero radiation loss at $\Delta T=0$.

The development of the analytic solution is based upon methodologies as contained in [Ozisik] and begins with classical expression for heat conduction in one dimension given by Equation (4).

$$\frac{\partial^2 T}{\partial x^2} = \frac{1}{\alpha}\frac{\partial T}{\partial t} \tag{4}$$

$$\alpha = \frac{k}{\rho c_p} \tag{4a}$$

$k$ = thermal conductivity [W / m·K]
$\rho$ = density [Kg / $m^3$]
$c_p$ = constant-pressure specific heat [J / Kg·K]

The above equation is solved subject to the boundary conditions and terms given in Equation (5).

$$k\frac{\partial T}{\partial x} + A_1 T = B_1 \quad (@x = L) \tag{5a}$$

$$-k\frac{\partial T}{\partial x} + A_2 T = B_2 \quad (@x = 0) \tag{5b}$$

$$A_i = m_i + h_i \tag{5c}$$

$$B_1 = -b_1 + Q_S + T_{A1}\left(m_1 + h_1\right) \tag{5d}$$

$$B_2 = -b_2 + T_{A2}\left(m_2 + h_2\right) \tag{5e}$$

$T_{Ai}$ = air temperature for surface i [K]
$h_i$ = convective heat transfer coefficient for surface i [W / $m^2$·K]
$m_i$ = slope of net radiation exchange curve for surface i
$b_i$ = intercept of net radiation exchange curve for surface i
$L$ = facet thickness [m]

An analytic solution for the system of Equations (4) and (5) is found as follows: treat this system as one for which the time variable in the boundary conditions is treated as an independent parameter separate from the time variable in the governing partial differential equation (i.e., Equation (4)). The resulting 'auxiliary' system with 'constant' (temporal) boundary conditions can then be readily solved, typically by separation of variables. This solution is then transformed to a complete time and spatial temperature expression using Duhamel's Theorem (Equation (12)) as given in [Ozisik] which relates the solution of this auxiliary system to the original system.

As an example consider a 1D slab with boundary conditions as given by Equation (5). We initially treat the $A_i$ and $B_i$ in Equation (5) as constants. This problem can then be split into steady-state and homogenous components. The steady-state component is

$$\frac{\partial^2 T_{SS}}{\partial x^2} = 0 \tag{6a}$$

with boundary conditions as given in Equations (5a) and (5b), and the homogenous component is

$$\frac{\partial^2 T_h}{\partial x^2} = \frac{1}{\alpha}\frac{\partial T_h}{\partial t} \tag{6b}$$

$$k\frac{\partial T_h}{\partial x} + A_1 T_h = 0 \quad (@x = L, t > 0) \tag{6c}$$

$$-k\frac{\partial T_h}{\partial x} + A_2 T_h = 0 \quad (@x = 0, t > 0) \tag{6d}$$

$$T_h(x,0) = T_0(x) - T_{SS}(x) \tag{6e}$$

Here $T_0(x)$ is the initial temperature distribution in the slab, and the solution for the original problem is Equation (6f).

$$T(x,t) = T_h(x,t) + T_{SS}(x) \tag{6f}$$

Equation (6a) has general solution as expressed in Equation (7).

$$T_{SS}(x) = A_0 x + B_0 \tag{7}$$

$$A_0 = \frac{A_2 B_1 - B_2 A_1}{k\left(A_1 + A_2\right) + A_1 A_2 L} \tag{7a}$$

$$B_0 = \frac{B_1 + B_2 - A_1 A_0 L}{A_1 + A_2} \tag{7b}$$

Before solving for facet temperature, the roots $\beta_m$ of the transcendental expression Equation (8), arising out of the spatial component of separation of variables as applied to Equation (6b) through (6e), are needed. Note that the form of this transcendental equation is a direct consequence of the algebraic form of Equations (6c) and (6d) [Ozisik].

$$\tan(\beta_m L) = \frac{\beta_m\left(H_1 + H_2\right)}{\beta_m^2 - H_1 H_2} \tag{8}$$

$$H_i = \frac{A_i}{k} \tag{8a}$$

The expression for facet temperature for the auxiliary system for this example is then given in Equation (9).

$$T(x,t) = T_{SS}(x) + \sum_{m=1}^{\infty} e^{-\alpha\beta_m^2 t}\,\frac{X(\beta_m,x)}{N(\beta_m)}\int_0^L X(\beta_m,u)\left(T_0(u) - T_{SS}(u)\right)du \tag{9}$$

$$X(\beta_m,x) = \beta_m\cos(\beta_m x) + H_1\sin(\beta_m x) \tag{9a}$$

$$N(\beta_m) = \frac{1}{2}\left[\left(\beta_m^2 + H_1^2\right)\left(L + \frac{H_2}{\beta_m^2 + H_2^2}\right) + H_1\right] \tag{9b}$$

Performing the integration results in the expression given in Equation (10) under the assumption of a spatially constant $T_0$.

$$T(x,t) = T_{SS}(x) + \sum_{m=1}^{\infty} e^{-\alpha\beta_m^2 t}\,\frac{X(\beta_m,x)}{N(\beta_m)}\left[\left(T_0 - B_0\right)C_1 - A_0 C_2\right] \tag{10}$$

$$C_1 = \sin(\beta_m L) + \frac{H_1}{\beta_m}\left(1 - \cos(\beta_m L)\right) \tag{10a}$$

$$C_2 = \beta_m\left(\frac{L\sin(\beta_m L)}{\beta_m} + \frac{\cos(\beta_m L) - 1}{\beta_m^2}\right) + H_1\left(-\frac{L\cos(\beta_m L)}{\beta_m} + \frac{\sin(\beta_m L)}{\beta_m^2}\right) \tag{10b}$$

This development assumes that solar flux, air temperature, etc., are all temporally constant. If these parameters are taken as time varying, then the boundary conditions are correspondingly time varying. Thus the terms $A_0$ and $B_0$ in Equation (10) are also time dependent. Note that it is assumed that $h_i$ in Equation (5c) is not taken to be time dependent in this instance. This is because a time dependent $h_i$ would result in time dependent $H_i$ in Equation (8), leading to time dependent $\beta_m$ and $C_i$ in Equation (10), which would render this approach nearly useless. Expressing Equation (10) in a form suitable for application of Duhamel's Theorem results in Equation (11).

$$\Psi(x,t,\tau) = T_{SS}(x) + \sum_{m=1}^{\infty} e^{-\alpha\beta_m^2 t}\,\frac{X(\beta_m,x)}{N(\beta_m)}\left[\left(T_0 - B_0(\tau)\right)C_1 - A_0(\tau)C_2\right] \tag{11}$$

The time dependent facet temperature is found by applying Equation (12) (Duhamel's theorem) to Equation (11) to generate the 'inverse' transformation.

$$T(x,t) = \Psi(x,0,0) + \int_{\tau=0}^{t} \frac{\delta}{\delta t} \Psi(x, t-\tau, \tau) d\tau \tag{12}$$

From Equations (11) and (12) we find the expression for facet temperature as given by Equation (13).

$$T(x,t) = T_0 + \sum_{m=1}^{\infty} \left(-\alpha \beta_m^2\right) \frac{X(\beta_m, x)}{N(\beta_m)} \int_{\tau=0}^{t} e^{-\alpha \beta_m^2 (t-\tau)} \left[ \left(T_0 - B_0(\tau)\right) C_1 - A_0(\tau) C_2 \right] d\tau \tag{13}$$

Analytic integration of the above is possible depending mainly on the character of weather data involved. For example, Fourier analysis might be used to decompose real weather into sinusoidal components. The resulting product of rational sinusoidal and exponential functions as contained in Equation (13) may allow for analytic integration. Note that parameter $\beta_m$ in Equation (13) is dependent on both the slope of the radiation curves and the wind velocity as is evident from Equations (5c) and (8). The slope of the radiation curves appears to vary only over a relatively small range as is illustrated in Figure 2. Therefore the impact of radiation curve slope on the value of $\beta_m$ as found from Equation (8) is quite small. However, wind velocity variations can be quite large and therefore the impact on $\beta_m$ is such that the resulting values might need to be found and stored off line. Fortunately, for facets that are no more than moderately thick (values of $L$ for example that do not exceed 10 cm), it can be shown that only the single primary root is significant to the solution of Equation (13). The higher order roots, in view particularly of the 'squared' dependency as shown in Equation (13), can be safely neglected in thin surface computations for practical applications.

It was decided to employ synthetic weather in this exercise in view of the ease in controlling boundary conditions, particularly wind velocity. Cloudless conditions were assumed which justify the use of solar loading that is smoothly varying over the course of a day. Wind velocity was held constant so that $h_i$ are constant. Air temperature and relative humidity were taken as simple sinusoidal functions varying from 10-30 degrees Celsius and 50 to 90 percent respectively. Solar flux was assumed to have a maximum value of 1000 [W / $m^2$] at the Earth's surface.

The forgoing could certainly represent conditions found in mid-latitudes and should dramatically illustrate the use of the analytic approach and facilitate comparison with various algorithms and numerical methods.

The result of the simulation is illustrated in Figures 3 and 4. The predicted surface temperatures cover a 24 hour period for a vertical, east facing box surface and for the top surface of the box.

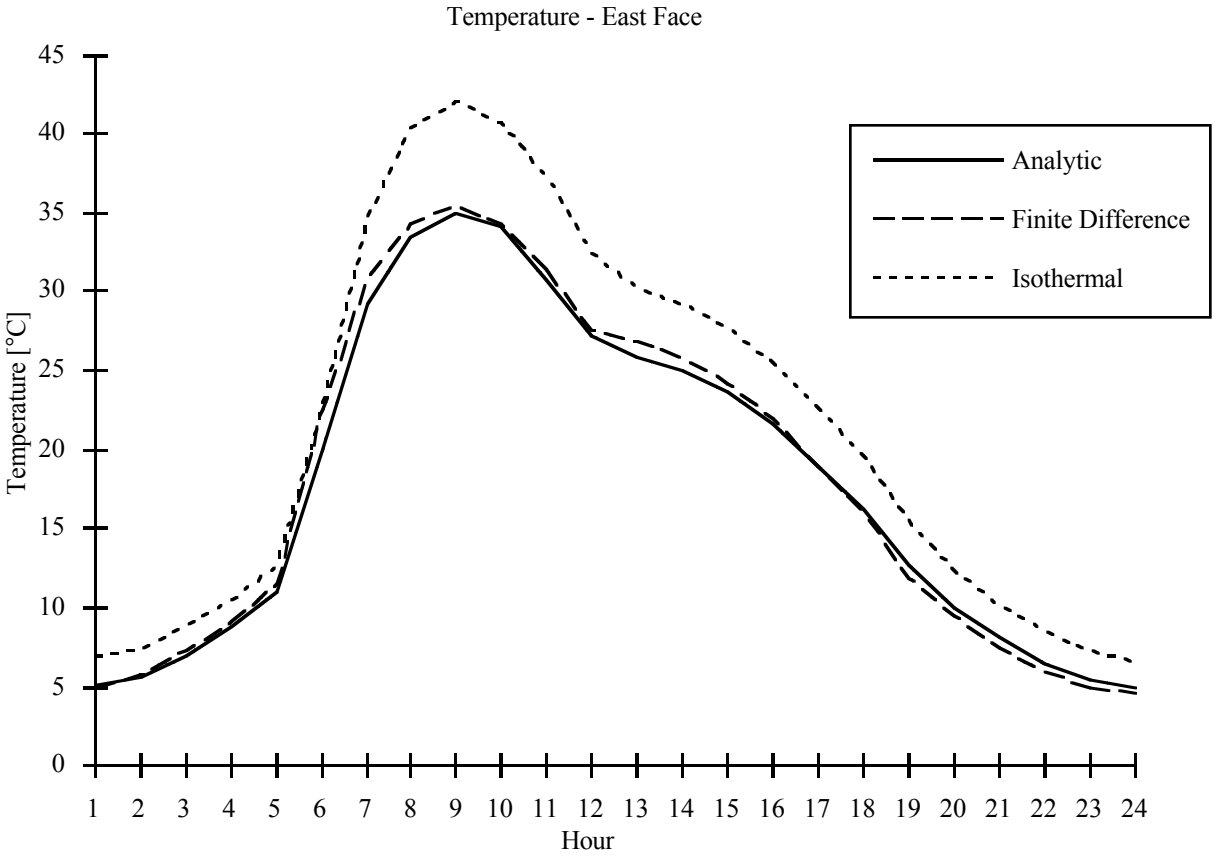


Figure 3: Comparison of the analytic method with two alternatives for predicting the surface temperature of an East facing vertical box side.

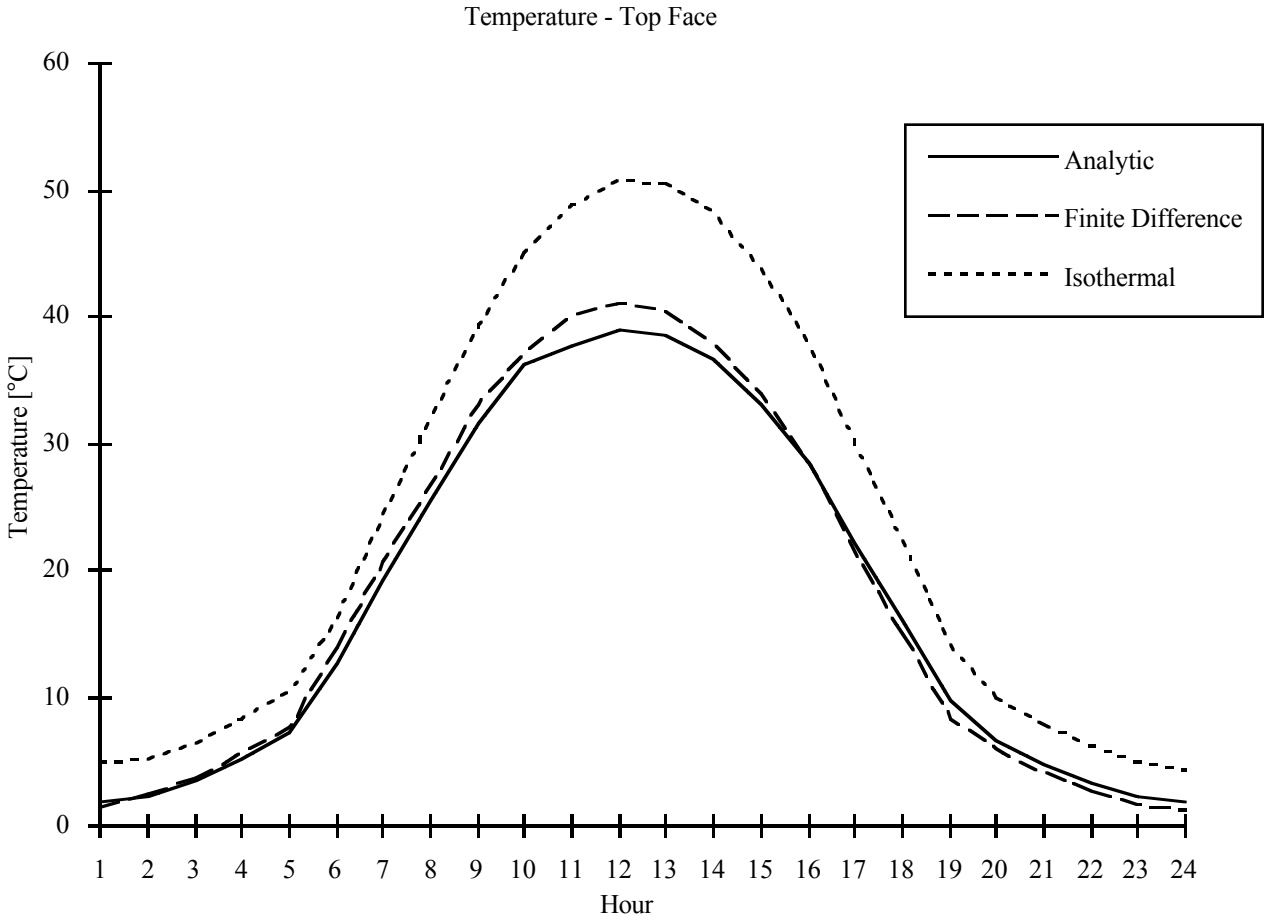


Figure 4: Comparison of the analytic method with two alternatives for predicting the surface temperature of the box top.

In the above figures, the analytic solution is compared with two numerical solutions. The first is based upon subdivision of the facet in the direction of heat flow into 3 intervals and using an explicit numerical solution with a 1 second time step (this small time step was required to maintain numerical stability). The other numerical solution assumes isothermal conditions for each facet.

The wall thickness of the box was chosen to be 1 centimeter (material: steel with olive green paint) which would represent a thin surface that would challenge the facility of standard numerical techniques for reliable temperature prediction. From both Figures 3 and 4 it is evident that the solution based upon the assumption of isothermal conditions differs significantly from solutions wherein sub-layering and conduction within the wall thickness is considered. Note further from the above figures that the explicit numerical and analytical solutions result in essentially the same predictions. The explicit solution represents a kind of control to insure accuracy of the analytic solution as outlined herein. It also further illustrates the influence of wall internal conduction upon the final temperature prediction. Note that with the low thermal inertia of the thin box wall that temperatures track the solar flux with no appreciable lag. The top face reaches its peak temperature at noon (Figure 4) whereas the vertical face reaches its peak temperature earlier in the morning hours when direct solar loading is maximized.

In the case of arbitrary initial temperature distribution $T_0(x)$ it becomes necessary to leave the spatial integral in Equation (9) unevaluated. The resulting expression for spatio-temporal temperature distribution in the slab then becomes Equation (14).

$$T(x,t) = T_0(x) + \sum_{m=1}^{\infty}\left(-\alpha\beta_m^2\right)\frac{X(\beta_m,x)}{N(\beta_m)}\int_{\tau=0}^{t} e^{-\alpha\beta_m^2(t-\tau)}\int_{u=0}^{L} X(\beta_m,u)\left(T_0(u) - T_{SS}(u,\tau)\right)du\,d\tau \tag{14}$$

$$T_{SS}(x,t) = A_0(t)x + B_0(t) \tag{14a}$$

The spatial integral in Equation (14) may be evaluated analytically provided $T_0(x)$ is of suitable form or can be decomposed into integrable basis components. Recall that it is still necessary to treat wind velocity as a constant in order to apply this equation. This would suggest that in the case of non-constant wind velocity time intervals $\Delta\tau$ be selected for which wind velocity is approximately constant and the equation applied to each time interval.

## 3. Conclusions

An analytic, 1D method for surface temperature prediction based upon time varying boundary conditions has been demonstrated. It is concluded that the analytic method as detailed herein is competitive with currently employed numerical techniques. Of course the analytic method offers the advantage of a direct solution at any time or position and does not necessitate the assumption of isothermal conditions where thin, highly conductive materials are employed. It may be used for surface temperature prediction for a feature of any complexity where facetization is employed in feature representation and 1D heat flow is justified. The difference in prediction where internal facet conduction is considered verses the assumption of isothermal conditions is demonstrated. The internal conduction is inherent in the analytic solution as outlined herein. Where numerical methods are employed, these results suggest that the use of sub-layering must be incorporated as part of the feature model, at least for high thermal conductivity surfaces.

It is further concluded that this analytic approach offers an excellent 'yardstick' against which to assess popular numerical approaches for accuracy where relatively simple geometric configurations permitting 1D heat flow assumptions arise.

With weather conditions that typically prevail at surface boundaries, numerical integration of Equations (13) or (14) will probably be required. However, basis functions may be found (other than Fourier series) which would serve to decompose weather parameter and initial temperature profiles in a manner that would permit analytic integration. This would seem worthy of further investigation.

The extension of this method to a full 3D solution is probably feasible and would encompass transverse conduction and internal radiation exchange.

## ACKNOWLEDGMENTS

This research was supported in part by AFOSR grant LRIR-93WL001.

## REFERENCES

[1] Ozisik, M. Necati, Heat Conduction, John Wiley & Sons, 1980.

[2] Blakwesiee, Leanne and Leonard J. Rodriguez, Technical Reference Guide For TCM2, Electro-optics & Physical Sciences Laboratory, Georgia Tech Research Institute, July 1993.

[3] Prism 3.1 User's Manual, Keweenaw Research Center, Michigan Technological University, June 1993.